Defining the *Protein Complex Proteome* of Plant Mitochondria[1][W]

Jennifer Klodmann, Michael Senkler, Christina Rode, and Hans-Peter Braun*

Institute for Plant Genetics, Faculty of Natural Sciences, Leibniz Universität Hannover, D–30419 Hannover, Germany

A classical approach, protein separation by two-dimensional blue native/sodium dodecyl sulfate-polyacrylamide gel electrophoresis, was combined with tandem mass spectrometry and up-to-date computer technology to characterize the mitochondrial "protein complex proteome" of Arabidopsis (*Arabidopsis thaliana*) in so far unrivaled depth. We further developed the novel GelMap software package to annotate and evaluate two-dimensional blue native/sodium dodecyl sulfate gels. The software allows (1) annotation of proteins according to functional and structural correlations (e.g. subunits of a distinct protein complex), (2) assignment of comprehensive protein identification lists to individual gel spots, and thereby (3) selective display of protein complexes of low abundance. In total, 471 distinct proteins were identified by mass spectrometry, several of which form part of at least 35 different mitochondrial protein complexes. To our knowledge, numerous protein complexes were described for the first time (e.g. complexes including pentatricopeptide repeat proteins involved in nucleic acid metabolism). Discovery of further protein complexes within our data set is open to everybody via the public GelMap portal at www.gelmap.de/arabidopsis_mito.

The proteome of Arabidopsis (*Arabidopsis thaliana*) mitochondria has been extensively characterized by gel-based and gel-free strategies (Kruft et al., 2001; Millar et al., 2001; Heazlewood et al., 2004, 2007; Lee et al., 2011; Taylor et al., 2011). Based on these projects, more than 500 proteins were assigned to mitochondria in Arabidopsis. However, targeting prediction software tools assign more than 1,500 proteins encoded by the Arabidopsis genome to this subcellular compartment. Therefore, it is concluded that most mitochondrial proteins, especially those of low abundance and/or high hydrophobicity, remain to be discovered. Many mitochondrial proteins form part of protein complexes (e.g. the complexes of the respiratory chain). However, again, only the complexes of high abundance could be characterized, while the ones of low abundance so far are not known.

Two-dimensional (2D) blue native (BN)/SDS-PAGE represents an alternative gel-based approach to analyze the mitochondrial proteome. Native gel electrophoresis is used for the first gel dimension to separate protein complexes, which are resolved into their subunits on a second gel dimension in the presence of SDS (Schägger and von Jagow, 1991). BN/SDS-PAGE is an ideal gel system for the analysis of protein complexes. At the same time and in contrast to the conventional 2D isoelectric focusing/SDS-PAGE system, detection of hydrophobic proteins is facilitated. The only disadvantage of BN/SDS-PAGE is a slightly reduced resolution of the resulting gels. Therefore, BN/SDS-PAGE was not used for broad-scale identification of proteins from plant mitochondria so far. The BN/SDS-PAGE analyses published to date allowed the identification of limited sets of proteins forming part of the mitochondrial proteome of potato (*Solanum tuberosum*; Jänsch et al., 1996 [16 proteins]; Bykova et al., 2003a [eight proteins]), Arabidopsis (Werhahn and Braun, 2002 [14 proteins]; Giegé et al., 2003 [26 proteins]), rice (*Oryza sativa*; Heazlewood et al., 2003b [57 proteins]; Millar et al., 2004b [18 proteins]), and *Arum maculatum* (Sunderhaus et al., 2010 [nine proteins]). Furthermore, 2D BN/SDS-PAGE was extensively used to systematically analyze subunits of individual protein complexes of plant mitochondria, like complex I (Heazlewood et al., 2003a; Millar et al., 2003; Sunderhaus et al., 2006; Meyer et al., 2007, 2008; Klodmann et al., 2010; Klodmann and Braun, 2011), complexes II and IV (Eubel et al., 2003; Millar et al., 2004a; Huang et al., 2010), complex III (Meyer et al., 2008), complex V (Heazlewood et al., 2003c; Meyer et al., 2008), the $I+III_2$ supercomplex (Peters et al., 2008), the formate dehydrogenase complex (Bykova et al., 2003b), and the TOM complex (Jänsch et al., 1998; Werhahn et al., 2001, 2003).

Meanwhile, mass spectrometry (MS) and appendant software tools have much improved. Therefore, we decided to reuse BN/SDS-PAGE for a first broad-scale proteomic analysis of plant mitochondria based on this experimental system. Overall, 471 unique proteins

[1] This work was supported by the Deutsche Forschungsgemeinschaft (grant no. Br 1829/10–1).

* Corresponding author; e-mail braun@genetik.uni-hannover.de.

The author responsible for distribution of materials integral to the findings presented in this article in accordance with the policy described in the Instructions for Authors (www.plantphysiol.org) is: Hans-Peter Braun (braun@genetik.uni-hannover.de).

[W] The online version of this article contains Web-only data.
www.plantphysiol.org/cgi/doi/10.1104/pp.111.182352

were identified in 200 gel spots excised from a single BN gel. The new 2D gel presentation software tool GelMap was further developed to allow a systematic exploration of the "protein complex proteome" of plant mitochondria. Evidence for the occurrence of at least 35 different protein complexes in Arabidopsis mitochondria is presented, several of which are described, to our knowledge, for the first time (e.g. protein complexes including the plant-specific pentatricopeptide repeat (PPR) proteins). The protein complex proteome of Arabidopsis mitochondria as defined by our study so far consists of more than 200 distinct proteins. Results of our investigation are presented at www.gelmap.de/arabidopsis_mito.

RESULTS AND DISCUSSION

Separation of Mitochondrial Proteins from Arabidopsis by 2D BN/SDS-PAGE

Mitochondrial fractions of 10 independent mitochondrial isolations from Arabidopsis cell suspension cultures were separated by 2D BN/SDS-PAGE as described in "Materials and Methods." The resulting gels were highly reproducible, as revealed by gel comparisons using the Delta 2D 4.2 software package (data not shown). A typical gel (Fig. 1) was selected for further analyses. The most prominent 200 spots were excised and analyzed by electrospray tandem MS. On average, six different proteins were identified per spot. Identifications were accepted if supported by MS reliability scores (Mascot) and by at least two matching peptides per protein (for details, see Supplemental Table S1). However, in some cases, single peptide hits were accepted for identification if other lines of evidence were present (e.g. data from previous publications). Primary data of all MS identifications are available in Supplemental Table S1 and at www.gelmap.de/arabidopsis_mito (at this site, tables are accessible directly by clicking the table symbol in the top right corner of the digital reference map). Overall, 1,160 proteins were identified within the 200 spots that represent 471 unique proteins. For all spots, values for apparent molecular mass were determined based on a precise scaling of the 2D BN/SDS gel as given in Figure 2.

Evaluation of Organelle Purity

To assess the purity of mitochondrial fractions, the subcellular localizations of all identified proteins were evaluated using the Arabidopsis SubCellular Proteomic Database (SUBA II; http://suba.plantenergy.uwa.edu.au/). This database summarizes all experimental and computer prediction data for subcellular localizations of proteins in Arabidopsis (Heazlewood et al., 2005, 2007). Of the overall 200 analyzed gel spots, 194 of the "first hit" identifications (97%) represent mitochondrial proteins according to experimental evidence given in the SUBA II database (Supplemental Table S2.1). Evaluation of all 471 unique proteins by the SUBA II database is more complicated. Many proteins of this data set are of very low abundance and consequently have not been assigned to a subcellular localization by experimental data yet. Overall, experimental evidence for the subcellular localization of 23% of the unique proteins has not been obtained according to SUBA II (Supplemental Table S2.2). A total of 57% of the identified unique proteins represent known mitochondrial proteins, and another 20% are assigned to other cellular compartments like plastids (9%), peroxisomes (2%), or the plasma membrane (8%). However, most of the unassigned proteins are localized in mitochondria according to targeting prediction computer programs and therefore represent candidates for new constituents of this subcellular compartment. Furthermore, identifications of proteins assigned to other subcellular compartments in most cases are based on only a few peptides (resulting in a comparatively low MS reliability score), which indicates that these proteins are of rather low abundance in our fraction. Therefore, evaluation of our MS data set using SUBA II was repeated based on the identified peptides of all proteins (Supplemental Table S2.3). Of the overall 6,992 peptides, 6,204 peptides belong to known mitochondrial proteins (89%). A comparatively low number of 346 peptides (5%) are assigned to known nonmitochondrial proteins. Another 442 peptides (6%) are of unknown subcellular localization

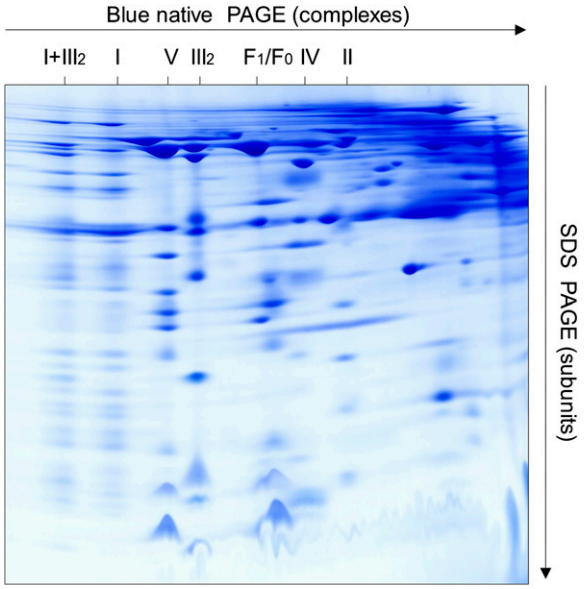

Figure 1. Analysis of the mitochondrial proteome of Arabidopsis by 2D BN/SDS-PAGE. Freshly isolated mitochondria (1 mg of mitochondrial protein) were solubilized by digitonin (5 g detergent g^{-1} protein), supplemented with Coomassie blue and loaded onto the 2D gel system. After electrophoresis, the gel was stained by Coomassie blue-colloidal. The identity of the OXPHOS complexes is given above the gel. $I+III_2$, Supercomplex composed of complex I and dimeric complex III; I, complex I; V, complex V (ATP synthase); III_2, dimeric complex III; F_1, F_1 part of ATP synthase; F_0, F_0 part of ATP synthase; IV, complex IV; II, complex II.

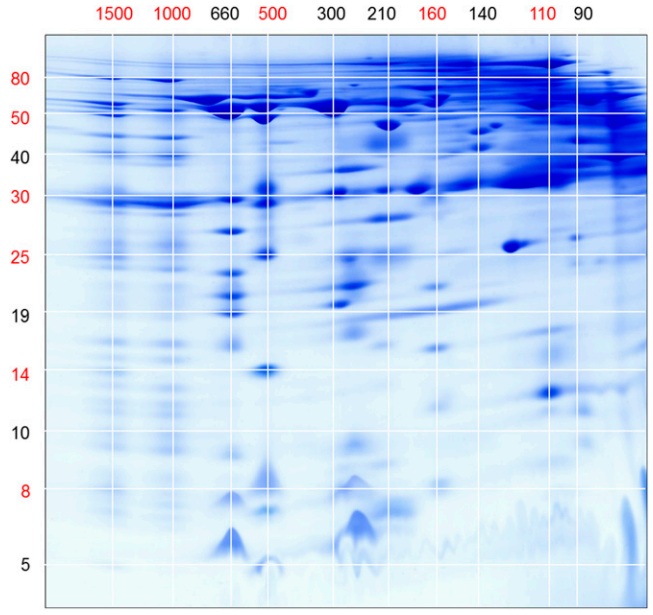

Figure 2. Molecular mass scale for the gel shown in Figure 1. The numbers refer to molecular masses (in kD). Masses used for calibration are given in red. BN gel dimension (horizontal) is as follows: I+III$_2$ supercomplex (1,500 kD), complex I (1,000 kD), dimeric complex III (500 kD), complex II (160 kD), and aconitate hydratase (110 kD). SDS gel dimension (vertical) is as follows: 75-kD subunit of complex I (spot 171), α-MPP (52 kD; spot 47), prohibitin (30 kD; spot 175), FeS subunit of complex III (23 kD; spot 53), QCR7 subunit of complex III (14 kD; spot 54), and the QCR8 subunit of complex III (8 kD; spot 56). Masses between those used for calibration were calculated with Eureqa software (version 0.83 β; www.eureqa.com).

because experimental data are lacking so far. However, most of the corresponding proteins are predicted to be localized in mitochondria (Supplemental Table S3). Therefore, the unassigned peptides/proteins represent candidates for newly identified mitochondrial proteins. Based on the different evaluation results, we finally concluded that our organellar fraction has a purity in the range of 93% to 95%.

Annotation of the Protein Complex Proteome of Arabidopsis Mitochondria

The novel GelMap annotation software package was used for online data presentation. GelMap was recently developed to functionally annotate 2D isoelectric focusing/SDS gels (Rode et al., 2011). The original software proved not to be suitable for the annotation of 2D BN/SDS gels because spots in general include several different proteins. Therefore, we upgraded the application range of GelMap for the assignment of lists of proteins to individual spots. Since all proteins are annotated according to distinct functions and protein complexes, the software now allows one to selectively display unknown protein complexes based on the vertical positioning of their subunits on a 2D BN gel.

For GelMap annotation, the image file of the 2D BN/SDS gel (Fig. 1) was loaded into the Delta 2D 4.2 software package for automated spot detection. A spot coordination (coord) file was generated by Delta 2D and exported into Excel. This Excel coord table was extended by several columns to add further details for all 1,160 identified proteins, like statistical values (Mascot score, number of peptides, coverage), biological values (calculated molecular mass, apparent molecular mass on the first gel dimension [native conditions] and the second gel dimension [denaturing conditions]), protein accession number, protein name, assignment to a protein complex and to a physiological process and to a subcellular compartment (Table I; Supplemental Table S1). The image file and coord table were both loaded into GelMap at www.gelmap.de. The how-to area of the GelMap Web site provides all information necessary to prepare and upload a data set (http://gelmap.de/howto). Based on the GelMap software package, the content of the columns of the coord table is automatically displayed on the map in pop-ups linked to the spots or in a menu to the right of the gel image, which includes information concerning the assignment of the proteins to protein complexes or functional categories (Fig. 3; Supplemental Fig. S2). By clicking on a spot, names of all included proteins and their MS reliability scores are listed in a pop-up window (Fig. 4), and by clicking on a protein name, further information is displayed, including a "more protein details" link at the bottom, which gives access to the coord table, including all information available for the protein of interest. A "more peptide details" link leads to a second table indicating peptide-specific information (e.g. ion score of a peptide, its amino acid sequence, and its modifications). In case a spot only includes a single protein, the additional information pop-up is displayed directly. Features best can be followed if directly tested on the Internet (www.gelmap.de/arabidopsis_mito). Proteins detected within the same spot are sorted according to their Mascot scores (column 2 in Supplemental Table S1). In general, we interpret that high scores (resulting from high scores for the identified peptides and/or many identified unique peptides) reflect high abundance of a protein. However, this assumption is not always correct, because the Mascot scores also depend on the biochemical properties of proteins.

The Protein Complex Proteome of Arabidopsis Mitochondria

The annotation of the Arabidopsis mitochondrial proteome as generated by GelMap offers several advantages. First of all, it allows easy access to protein identification data of large proteome data sets based on functional categorization. But more importantly, it specifically allows searching for protein complexes of low abundance, which are positioned at the same location on the gels as protein complexes of high abundance, like the complexes of the oxidative phosphorylation system. The low-abundance protein complexes in most cases have comparatively low MS

Table I. *Column content of the results table presented in* Supplemental Table S1

Column (from Left to Right)	Content	Comment
1	Spot number	Spot number on the 2D BN/SDS gel (Figure 3)
2	Mascot score	Probability score for the protein identification (www.matrixscience.com)
3	No. of peptides	No. of unique peptides matching to a protein hit
4	Coverage	Sequence coverage of a protein by the identified peptides
5	Calculated molecular mass	Calculated molecular mass of the protein (note that in many cases, presequences are cleaved off from nucleus-encoded mitochondrial proteins after their transfer into mitochondria is completed; as a consequence, the apparent molecular mass is 1–8 kD smaller than predicted)
6	Apparent molecular mass, second dimension	Apparent molecular mass as determined on the second gel dimension (for mass determination, see Fig. 2)
7	Apparent molecular mass, first dimension	Apparent molecular mass as determined on the first gel dimension (for mass determination, see Fig. 2)
8	Accession number, Arabidopsis Genome Initiative	Accession numbers according to the TAIR database (http://www.arabidopsis.org/); numbers are linked to protein entries of the TAIR database
9	Name of protein	
10	Protein complex	Assigned mitochondrial protein complex (in many cases according to precise location on the same vertical line on the 2D BN/SDS gel)
11	Physiological category	Seven categories were defined: (a) oxidative phosphorylation; (b) pyruvate metabolism and TCA cycle; (c) transport; (d) protein folding and processing; (e) processing of nucleic acids; (f) other metabolic pathways; and (g) uncharacterized
12	Subcellular localization	Subcellular localization according to the SUBA II database (http://suba.plantenergy.uwa.edu.au/)
13	Database	Database used for protein identification (T = TAIR [http://www.arabidopsis.org/], database release 10)
14	Coordinate on the *x* axis	Generated by Delta 2D
15	Coordinate on the *y* axis	Generated by Delta 2D
16	Spot number	Copy of column 1 for better readability of the table

reliability scores, which nevertheless are clearly above the threshold. Using the categorization tools offered by GelMap, their positioning along a vertical line becomes visible, allowing one to deduce new protein-protein interactions. The following 35 protein complexes were found in the course of the project (for summary, see Table II).

The I+III$_2$ Supercomplex (1,500 kD) and Complex I (1,000 kD)

Subunits present within plant complex I recently were systematically characterized (Klodmann et al., 2010; Klodmann and Braun, 2011). Currently, 48 different subunits are known, seven of which occur in pairs of isoforms. In the frame of our study, 44 subunits were detected in monomeric complex I. Four subunits were not found (ND4L [AtMg00650], 13-kD subunit [At3g03070], and the plant-specific subunits At5g14105 and At1g68680). Subunit ND4L was never identified in any proteomic study, probably due to its extreme hydrophobicity. The plant-specific subunit At1g68680 (8.3-kD protein), which was described by Meyer et al. (2008), is present on our 2D gel map but at a position far away from complex I (spot 168; 60-kD range with respect to the native gel dimension). It could have been detached from complex I during solubilization, or it may represent an erroneously identified complex I subunit. Most of the identified subunits of complex I also were found in the 1,500-kD I+III$_2$ supercomplex.

Four additional proteins were discovered in our study, which represent candidates for newly identified complex I subunits: At3g10110 (spot 17), At1g18320 (spot 186), At1g72170 (spots 149 and 151), and At2g28430 (spot 154). The first two subunits represent isoforms and resemble proteins of the TIM preprotein translocase family. Interestingly, another complex I subunit, the so-called "B14.7" protein, exhibits similarity to the proteins of the TIM family (Carroll et al., 2002). Three of the four new subunits were found both in the 1,500-kD supercomplex and in monomeric complex I, supporting their assignment as complex I subunits (one new subunit, At2g28430, was detected only in the supercomplex).

Complex I subunits were additionally detected in 27 spots not forming part of the vertical rows of spots representing the I+III$_2$ supercomplex or monomeric complex I. All these subunits migrate on the second gel dimension at a lower molecular mass than on the first gel dimension. At the same time, their MS reliability scores are low, most likely indicating their comparatively low abundance. Interestingly, several of these complex I subunits form part of vertical rows of

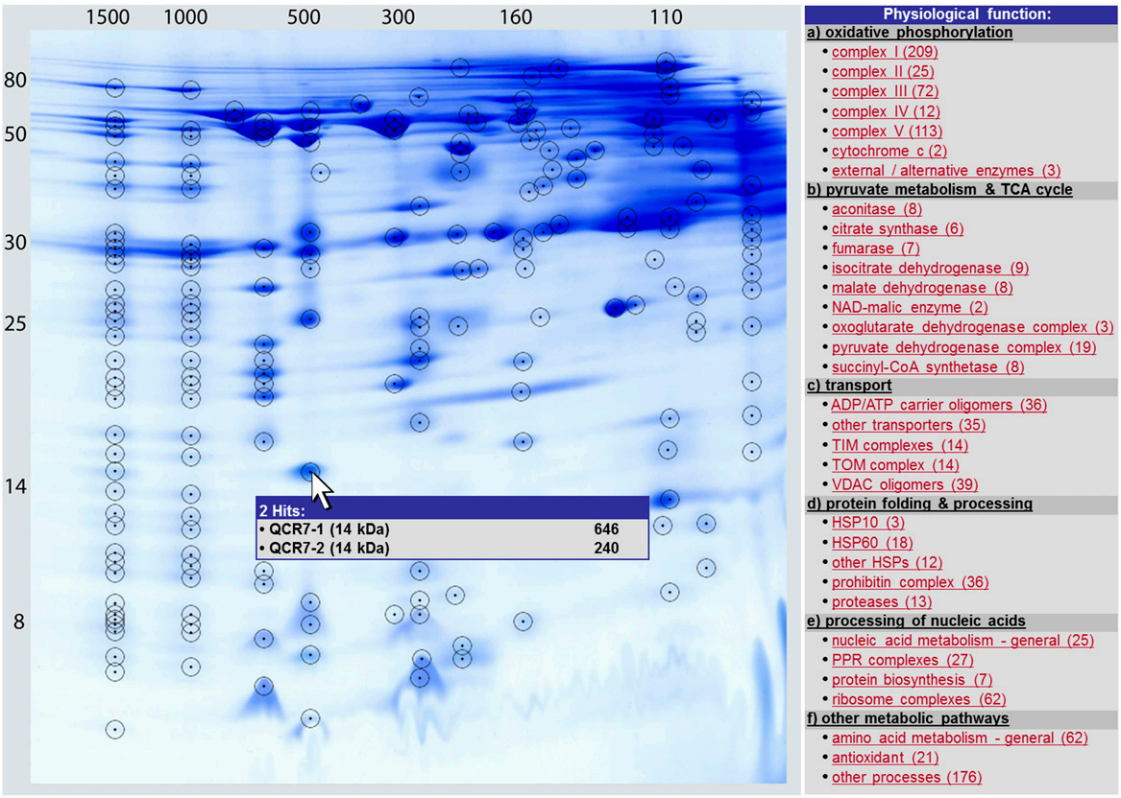

Figure 3. Reference map of the protein complex proteome of Arabidopsis mitochondria as presented in GelMap (www.gelmap.de/arabidopsis_mito). Protein spots identified by MS are circled. Most spots include multiple proteins. The menu to the right offers functional classifications of subunits according to physiological functions and protein complexes. The numbers in parentheses refer to the number of identified proteins per individual complex. Upon clicking on a protein complex, names of all its subunits become available (Supplemental Fig. S2). Detailed information on spots is given upon clicking on the encircled spots on the 2D image (see Fig. 4). The GelMap software package also has different search options (e.g. for a distinct protein by name or accession number). The search options are located beneath the menu to the right of the gel image (not shown here). For further features of GelMap, see www.gelmap.de/arabidopsis_mito.

spots on the 2D gel, indicating the presence of complex I breakdown products or assembly intermediates in our mitochondrial fraction. For instance, four complex I subunits of the membrane arm of complex I (Klodmann et al., 2010) were identified in vertical alignment close to the ATP synthase complex (650 kD). Also, in most other cases, the positions of complex I subunits separated from the holoenzyme nicely correlate with the positions of known complex I subcomplexes (Klodmann et al., 2010). This illustrates the suitability of the GelMap software tool to identify protein complexes of low abundance (e.g. assembly intermediates of OXPHOS complexes).

The ATP Synthase Complex (Complex V)

Based on our molecular mass calibration (Fig. 2), complex V runs at 660 kD on the native gel dimension. Fourteen subunits have been reported for Arabidopsis (Heazlewood et al., 2003c; Meyer et al., 2008), all of which are included in our map except for subunit c, which is small and very hydrophobic. Additionally, a homolog of subunit g from other groups of eukaryotes was detected in the low native mass range (14-kD protein; present in three isoforms: At4g29480, At2g19680, and At4g26210; spots 164 and 165). In yeast, this subunit only is associated with ATP synthase within the dimeric ATP synthase supercomplex (Arnold et al., 1998). Under the conditions applied during our investigation, ATP synthase dimers are not stabilized. Since subunit g is completely detached from the ATP synthase monomer on our 2D gel, it probably also represents a dimer-specific protein in Arabidopsis.

The more hydrophobic subunits of complex V, especially subunits a and b, were identified in several neighboring spots and therefore are difficult to precisely localize on our map. Our interpretation of the assignment of these subunits to the spots on the 2D gel is given in Supplemental Figure S1.

On our 2D gel (Fig. 1), the known F_1 and F_0 subcomplexes run at 300 and 260 kD. The relatively high abundances of these subcomplexes indicate that they represent breakdown products rather than assembly intermediates. F_1 includes subunits α, β, γ, δ, and ε, and F_0 includes subunits a, d, 8, OSCP, ATP17 (plant specific), and 6 (plant specific). The FAD subunit

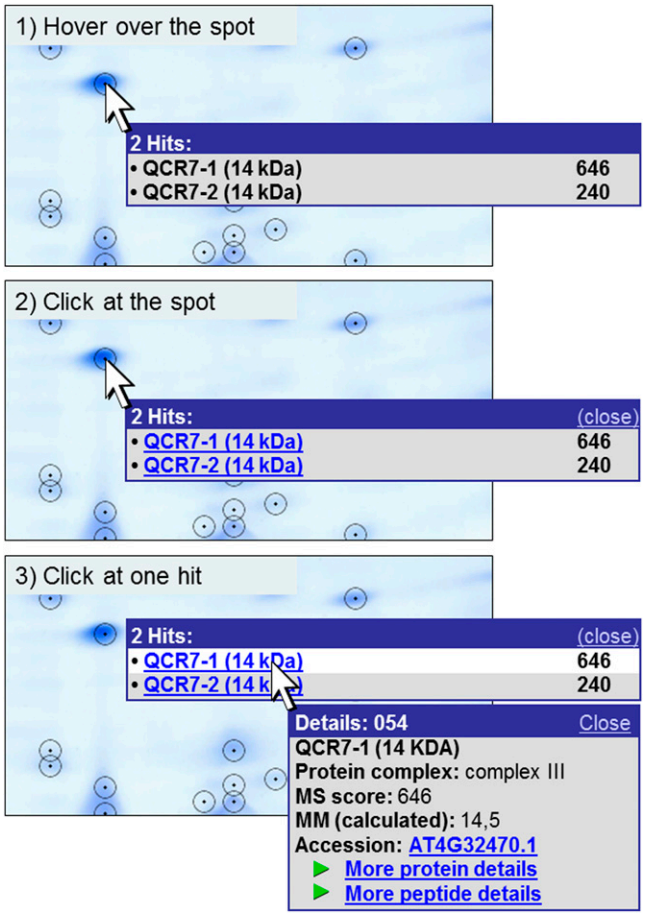

Figure 4. Pop-up function on the gel map. Information about the proteins identified in a spot can be viewed directly on the gel image. The user can hover over a spot (1) that opens a tooltip containing the names of all included proteins (left) as well as their MS reliability scores (right). By clicking on the spot (2), the window is fixed, and protein names are hyperlinked to more detailed information. Protein details become visible in a new window by clicking on the protein of interest (3). If only one protein is identified in a spot, the first click on the spot already opens the details window shown in 3. This window contains (from top to bottom): spot number (in the blue frame), protein name, dedicated protein complex, MS reliability score, the calculated molecular mass, and the Accession number (according to TAIR), which is linked to the respective entry on the TAIR homepage (www.arabidopsis.org). The "more protein details" link at the bottom of the details window is linked to a table showing all proteins identified in the respective spot (Supplemental Table S1). Besides the characteristics already given in the pop-up window, it contains further information about spot characteristics (such as coordinates and apparent masses), MS analysis, and the physiological context of the proteins (Table I). The "more peptide details" link leads to a table that includes details of the peptides identified by MS.

does not form part of the two subcomplexes but was only detectable within the holocomplex or as a singular protein (spots 132 and 133).

Subunits of complex V additionally were detected within several other spots not forming part of the vertical rows of spots representing the holocomplex or the F_1 and F_0 subcomplexes, especially in the low native mass range. These proteins may form part of smaller complex V subcomplexes or assembly intermediates.

Cytochrome *c* Reductase (Complex III; 500 kD)

This central complex of the OXPHOS system has 10 subunits in plants (Braun and Schmitz, 1995; Meyer et al., 2008), all of which are included in our map. For the first time to our knowledge, the so-called "hinge" subunit (QCR6) was detected for Arabidopsis. Six of the subunits are present in pairs of isoforms (α-MPP, cytochrome c_1, FeS protein, QCR6, QCR7, and QCR8). All 10 subunits also form part of the I+III_2 supercomplex. No subcomplexes of complex III were detected, further supporting its extraordinary stability (Heinemeyer et al., 2009).

Cytochrome *c* Oxidase (Complex IV)

On BN/SDS gels, complex IV usually is found in a larger (230 kD) and a smaller (200 kD) form. The smaller form lacks Cox VIb and possibly other subunits (Eubel et al., 2003). On our BN/SDS reference gel, complex IV is present in the smaller form. Its apparent molecular mass was determined to be 207 kD. For Arabidopsis, 14 different subunits were described, until now termed Cox I, Cox II, Cox III, Cox Vb, Cox Vc, Cox VIa, Cox VIb, Cox VIc, and Cox X1 to Cox X6 (Millar et al., 2004a). The Cox X1 to X6 subunits are plant specific. The map includes Cox II, Cox Vc, Cox X2, and Cox X4. The Cox I, Cox III, and Cox Vb subunits are visible on the gel but peptides could not be detected, most likely due to the extreme hydrophobicity of these proteins. Currently, further efforts are being made to identify these subunits and include them in the online version of GelMap. The Cox X6 subunit was found in gel regions representing larger native masses and therefore might only be included in the larger form of complex IV. Some of the complex IV subunits occur in two or more isoforms (Millar et al., 2004a), several of which were detected in the frame of our project.

Succinate Dehydrogenase (Complex II)

The holocomplex has a size of 160 kD and consists of eight subunits termed SDH1 to SDH8, four of which are plant specific (SDH5–SDH8; Eubel et al., 2003; Millar et al., 2004a). All these proteins except SDH8 are included in our map (SDH8 migrates at the dye front on the 2D BN/SDS gel). Some proteins occur in isoforms. All subunits except SDH5 also are present in a smaller form of complex II, which runs at about 100 kD. Analyses by BN PAGE revealed that complex II gets dissected into two subcomplexes that comigrate at this position on the native gel dimension (S. Sunderhaus and H.P. Braun, unpublished data).

Table II. *The protein complex proteome of Arabidopsis mitochondria*

Protein Complex	Apparent Molecular Mass[a]	Composition	No. of Different Subunits Included in the Map[b] (+No. of Additional Subunits Not Found in This Study)		Additional Isoforms[c]
	kD				
$I+III_2$ supercomplex	1,500	Heterooligomer	All subunits of complex I and III		–
Complex I	1,000	Heterooligomer	44 + 3[d]	(+4)	8
Prohibitin	1,000	Homooligomer	1		6
HSP60 complex	783	Homo-14-mer	1		5
Membrane arm, complex I	660	Heterooligomer	Approximately 35 subunits of complex I		–
Complex V	660	heterooligomer	14	(+1)	2
Complex III	500	Heterooligomer	10		6
PPR2 complex	369	Homooligomer (?)	1 + X		1
NAD malic enzyme	369	Heterohexamer	2		0
F_1 part of complex V	300	Heterooligomer	Five subunits of complex V		–
TOM complex	260	Heterooligomer	4	(+2)	6
F_0 part of complex V	260	Heterooligomer	Seven subunits of complex V		–
Clp protease complex	260	Homo-14-mer	1		0
Oxoglutarate DH-E1	210	Homodimer	1		1
PPR3 complex	209	Homooligomer (?)	1 + X		0
Lon protease	209	Homodimer	1		3
Glu dehydrogenase	209	Homohexamer	1		2
Complex IV	207	Heterooligomer	6	(+8)	8
Fumarase	200	Homotetramer	1		1
Complex II	160	Heterooligomer	7	(+1)	5
PPR1 complex	160	Homooligomer (?)	1 + X		0
Isocitrate DH	160	Homotetramer	1		3
Malate DH	160	Homotetramer	1		2
Alternative ND (NDA + NDB)	160	Heterotrimer	2		4
PPR5 complex	156	Homooligomer (?)	1 + X		1
Metaxin/SAM complex (?)	150	Heterooligomer	1		0
Arginase	150	Homotrimer	1		1
Pyruvate DH-E1	138	Heterotetramer	2		1
Isovaleryl-CoA dehydrogenase	132	Homotetramer (?)	1		0
TIM23 complex	115	Heterooligomer	2	(+4)	2
Citrate synthase	110	Homodimer	1		1
HSP10 complex	108	Homoheptamer	1		1
Voltage-dependent anion channel complexes	90/180	Homotri/hexamers	1		4
ADP/ATP translocase	60/120	Homodi/tetramers	1		2
TIM9-10 complex	86	Heterohexamer	2		0
Σ[e] (35 complexes)	86–1,500		118	(+20)	76

[a]Apparent molecular mass as determined in this study. [b]Without isoforms. [c]Based on the genome sequence. Note that not all isoforms were detected in the frame of this project. [d]Three new complex I subunits were discovered in the frame of this project. [e]Subunits detected in a holocomplex and in subcomplexes only were counted once.

Cytochrome *c*

The intermembrane space protein cytochrome *c*, which translocates electrons from complex III to complex IV, occurs as a monomer of 12 kD but also was detected in the native range of about 100 kD. It is positioned on a vertical line together with the cytochrome *c*-binding enzyme L-galactono-1,4-lactone dehydrogenase. We speculate that these two proteins form a protein complex of about 100 kD.

Alternative NAD(P)H Dehydrogenases

Alternative NAD(P)H dehydrogenases are encoded by two gene families in Arabidopsis termed NDA (two genes) and NDB (four genes; Michalecka et al., 2003). On our map, we found the NDA2, NDB2, and NDB4 proteins (spots 96 and 94). Molecular masses of the monomeric precursor proteins are in the range of 56 to 65 kD. All proteins were detected in the 160-kD range of the native gel dimension. Similar results were previously reported for NDA2 (Rasmusson and Agius, 2001). We postulate that the NDA and NDB proteins might form a protein complex that probably has a heterotrimeric structure.

Protein Complexes of Tricarboxylic Acid Cycle Enzymes

All enzymes of the tricarboxylic acid (TCA) cycle are included in our map. Due to horizontal and vertical smearing effects of the BN/SDS gel, most proteins

were identified within several spots. However, based on their Mascot scores, conclusions can be drawn concerning their main locations on the map. In accordance with reports in the literature, three enzymes, fumarase, isocitrate dehydrogenase, and malate dehydrogenase, have a homotetrameric structure (Table II). Citrate synthase most likely represents a homodimer (spot 118). Furthermore, the E1 subunit of the 2-oxoglutarate dehydrogenase complex forms a homodimer (spot 77). In contrast, aconitase can only be found as a monomer on the gel (spots 114 and 201). Succinyl-CoA synthetase consists of an α-subunit (spot 130) and a β-subunit (spots 119 and 202), but evidence for the interaction of these two subunits is not obvious in our map. Finally, as reported above, succinate dehydrogenase (complex II of the respiratory chain) is a heterooligomer composed of eight distinct subunits in plants. Most TCA cycle enzymes are present in multiple isoforms. It currently cannot be decided if the homooligomeric TCA cycle protein complexes are composed of multiple copies of identical or distinct isoforms. Further biochemical analyses are necessary to validate and characterize the new protein complexes identified by this approach.

Pyruvate Dehydrogenase Complex

Pyruvate dehydrogenase probably is the largest protein complex of the mitochondrial matrix. It is composed of numerous copies of the E1-α, E1-β, E2, and E3 subunits and has an overall molecular mass of about 9.5 MD (Zhou et al., 2001). The holoenzyme was outside of the molecular mass limit of our BN/SDS gel. However, subcomplexes were found. A tetramer composed of two E1-α (spot 110) and two E1-β (spot 104) subunits runs at about 140 kD on the native gel dimension (Table II). Furthermore, much larger protein associations were detected that include the E3 subunit (spots 3, 31, 96, and 172).

NAD Malic Enzyme

NAD malic enzyme forms a protein complex of about 370 kD (spot 59). It is composed of two distinct subunits of about 60 kD each. The protein complex, therefore, probably has a hexameric structure. In the literature, different oligomeric structures were reported for this enzyme complex that range from dimeric to octameric (Jenner et al., 2001).

The Preprotein Translocase of the Outer Mitochondrial Membrane (the TOM Complex)

The core of the TOM complex consists of six distinct subunits: TOM40, TOM20, TOM22 (TOM9), TOM7, TOM6, and TOM5 (Werhahn et al., 2001, 2003). Its native molecular mass is 260 kD on our 2D gel, slightly smaller than reported before. All subunits are included in our map, except for the very small TOM5 and TOM6 proteins, which migrate within the dye front of the second dimension gel. The preprotein receptor TOM20 occurs in several isoforms. One protein of unknown function comigrates with the TOM complex on the 2D gel (At3g49240; spot 62). It has a size of 70.2 kD and contains a tetratricopeptide motif like the TOM70 preprotein receptor, which was characterized for fungal and mammalian mitochondria. It currently cannot be decided if this protein physically interacts with the TOM complex in Arabidopsis. Metaxin (36 kD), another outer membrane protein involved in protein translocation, runs at 150 kD on the native gel dimension.

Preprotein Translocases of the Inner Mitochondrial Membrane (the TIM Complexes)

Four distinct TIM complexes are known, which are designated TIM22, TIM23, TIM9/10, and TIM9/13 complexes according to the protein components included (Lister et al., 2005, 2007). Only two of these complexes clearly were identified on our map: (1) the TIM 9/10 complex, which has a hexameric structure (three TIM9 and three TIM10 proteins; Baker et al., 2009), is located in the mitochondrial intermembrane space and runs at about 86 kD on the BN gel dimension; and (2) the TIM23 complex, which runs at about 110 kD and includes at least the TIM17 and TIM44 subunits. Another TIM complex, which includes the TIM21 protein, runs at about 150 kD. TIM21 represents a nonessential subunit of the TIM23 complex. Its binding partners were not identified in the course of our study. As already mentioned above, two subunits resembling TIM proteins form part of complex I and the $I+III_2$ supercomplex in plants (At3g10110/At1g18320 and At2g42210; spots 17, 186, 147, and 148).

The ADP/ATP Translocase and Other Members of the Mitochondrial Metabolite Carrier Family

The ADP/ATP translocase runs at 30 kD on the second gel dimension. On the native gel dimension, it smears from 30 kD to about 1,500 kD. However, highest Mascot scores clearly are in the 60- to 120-kD range, indicating dimeric to tetrameric structures. Several isoforms occur that may be combined or separated within the oligomers. The ADP/ATP translocase is known to have a large N-terminal extension that is removed upon import but dispensable for protein targeting (Emmermann et al., 1991; Winning et al., 1992; Mozo et al., 1995). Possibly, this precursor protein should be considered to represent a polyprotein that is cleaved into two separate polypeptides, the smaller of which is of unknown function. Similar to the results obtained for the ADP/ATP translocase, other members of the mitochondrial metabolite carrier family were predominantly found in the 60- to 120-kD region (e.g. members of the dicarboxylate and tricarboxylate carrier subfamilies, the phosphate translocase, and the plant uncoupling protein).

Porin Complexes

"Porin" of the outer mitochondrial membrane, which is designated the "voltage-dependent anion channel" of mitochondria, runs at 30 kD on the second gel dimension and is widely distributed on the native gel dimension between 30 and 1,500 kD. Spots with highest Mascot scores are at about 100 and 180 kD, indicating that porins most likely form trimers that might associate to form hexamers.

Heat Stress Protein Complexes

The HSP60 complex is composed of two heptameric rings of HSP60 monomers. Its native molecular mass is close to 800 kD. In the presence of ATP, two heptameric HSP10 rings bind to the HSP60 complex. Since 2D BN/SDS-PAGE was carried out in the absence of ATP, the HSP10 heptamers are dissociated and form an extra protein complex of about 100 kD.

Prohibitin Complex

Prohibitin forms large ring-like protein complexes that are assumed to have functional importance as chaperones for the protein complexes of the oxidative phosphorylation system (Van Aken et al., 2010). The main form of this protein complex migrates between 900 and 1,100 kD on the native gel dimension. Five different isoforms (prohibitin 1, 2, 3, 4, and 6) were detected in our 2D map.

Protease Complexes

In plants, the heterodimeric mitochondrial processing peptidase forms part of complex III (Braun et al., 1992; see above). Two further protease complexes were detected in our 2D map: the clp protease complex at 260 kD (spot 194), which is composed of 14 clp monomers (Halperin et al., 2001; Peltier et al., 2004), and a putative homodimeric Lon protease complex at 209 kD (spot 77).

Protein Complexes of Mitochondrial Amino Acid Metabolism

The Glu dehydrogenase complex (spots 80 and 81) runs at 209 kD and probably has a homotetrameric structure. An arginase complex runs at 150 kD (spot 103) and probably is represented by a homotrimer. The 40-kD isovaleryl-CoA dehydrogenase (spot 101) runs at 132 kD and probably forms a trimer or tetramer. The Gly dehydrogenase complex is of high abundance in mitochondria isolated from green tissue but of low abundance in nongreen cell cultures. It consists of the T, P, L, and H subunits (Douce et al., 2001). The P and L proteins are part of our map but do not form a protein complex. Hence, the complex seems to be destabilized under the conditions applied.

PPR Protein Complexes

PPR proteins represent a large protein family that especially occurs in plant organelles. They are involved in RNA maturation processes like RNA splicing or editing (Delannoy et al., 2007). Twenty-seven PPR proteins were detected in our map, several of which obviously form part of protein complexes because they run on the native gel dimension much higher than explainable by their monomeric molecular mass. For instance, (1) PPR1 (spot 94, Mascot score 855, 70 kD) runs at 160 kD; (2) PPR2-1 and PPR2-2 (spot 95, Mascot scores 129 and 106, 67 kD) both run at 396 kD; (3) PPR3 (spot 80, Mascot score 447, 50 kD) runs at 209 kD; and (4) PPR5-1 (spot 98, Mascot score 114, 46 kD) runs at 156 kD. Further experimental evidence is necessary to determine the exact composition of these PPR protein complexes. It currently cannot be decided whether these complexes have homooligomeric or heterooligomeric subunit composition.

Further Proteins and Protein Complexes

Many further enzymes listed under "other metabolic pathways" similarly migrate at a much higher position on the native gel dimension than on the denaturing gel dimension, indicating the presence of further protein complexes. It is beyond the scope of this publication to list all these discrepancies. However, our database is publicly accessible via the GelMap platform at www.gelmap.de/arabidopsis_mito and can be queried for any protein accession of interest. The database also includes several proteins that so far could not be experimentally assigned to a subcellular compartment. These proteins represent candidates for new mitochondrial components, but their subcellular localization should be evaluated by further studies.

The presented reference map allows, to our knowledge for the first time, a systematic definition of the mitochondrial protein complex proteome. The protein complexes described in this study refer to Arabidopsis mitochondria isolated from dark-grown suspension culture cells. Analyses of other tissues of this model plant as well as analyses of Arabidopsis plants cultivated in varying conditions surely will reveal differing results. Changes in the abundance of protein complexes will be analyzed in the future, and the results will be implemented into the GelMap project.

The identification of protein complexes by the combination of 2D BN/SDS-PAGE, tandem MS, and GelMap provides comprehensive insights into the plant mitochondrial protein complex proteome. Many protein complexes could be identified for the first time. Biochemical studies will follow to validate the presence and composition of these protein complexes in the future.

CONCLUSION

Our study allowed us to identify 471 distinct proteins on a 2D BN/SDS gel and to assign more than 150

of these proteins to 35 different mitochondrial protein complexes. Due to the application of BN/SDS-PAGE, hydrophobic proteins are not discriminated. Therefore, broad-range insights into the protein complex proteome of plant mitochondria have been possible. Several protein complexes were described for the first time (e.g. complexes including the plant-specific PPR proteins). Nevertheless, our experimental strategy to identify protein complexes has to be considered to represent a biased approach, because the 200 most abundant spots were selected for MS analysis, and thereby protein complexes of low abundance only were detected if positioned at a gel region of a protein complex of high abundance. If the protein complex proteome of plant mitochondria is completely analyzed, it would be necessary to systematically scan a 2D BN/SDS gel by MS (e.g. within 100 horizontal gel stripes by 100 spots each [=10,000 spots]). In principle, such an analysis would be feasible, and annotation by GelMap would allow visualizing all protein complexes above the detection limit for MS-based protein identifications. Already for the study presented here, the GelMap software package proved to be very helpful for the exploration of a 2D BN/SDS gel. Its option to differentially display protein complexes should be of increased value for evaluating BN/SDS gels of nonmitochondrial fractions, because resolution of the resulting gels often is of lower quality. We believe that GelMap in general will prove to be a valuable tool for gel-based proteomics.

MATERIALS AND METHODS

Preparation of Mitochondria and 2D BN/SDS-PAGE

Mitochondria were isolated from Arabidopsis (*Arabidopsis thaliana*) cell suspension cultures as described by Werhahn et al. (2001). Organelle fractions were divided into aliquots of 100 μL (10 μg mitochondrial protein μL^{-1}). For sample preparation prior to BN PAGE, freshly prepared organelles of one aliquot were sedimented by centrifugation for 10 min at full speed (Eppendorf centrifuge) and resuspended in 100 μL of digitonin solubilization buffer (30 mM HEPES, 150 mM potassium acetate, 10% [v/v] glycerol, and 5% [w/v] digitonin). After incubation for 10 min on ice, insoluble material was discarded by another centrifugation step (10 min, full speed, Eppendorf centrifuge), and the supernatant was supplemented with 5 μL of Coomassie blue solution (750 mM aminocaproic acid, 5% [w/v] Coomassie blue 250 G). Fractions were directly loaded onto a BN gel. BN gel electrophoresis was carried out as described before (Wittig et al., 2006). Basic parameters were as follows: (1) Protean II electrophoresis chamber (Bio-Rad); (2) gel dimensions of 16 × 16 cm; (3) polyacrylamide concentration of the first dimension gradient gel, 4.5% to 16% (top to bottom); and (4) second gel dimension, Tricine SDS-PAGE system (Schägger and von Jagow, 1987), constant polyacrylamide concentration on the separation gel (16.5%), which was overlaid with a 2.5-cm spacing gel as described by Jänsch et al. (1996). Gels were stained according to the Coomassie blue-colloidal protocol (Neuhoff et al., 1988).

Protein Identification by MS

Spots were cut out from a 2D gel using a manual spot picker (Genetix; spot diameter, 1.4 mm) and were numbered consecutively from 1 to 200. In-gel digestion was carried out as described by Klodmann et al. (2010). Tryptic peptides were resolved in 22 μL of liquid chromatography (LC) sample buffer (2% acetonitrile and 0.1% formic acid in water), and 15 μL was injected into the LC-MS system. Nano-HPLC electrospray ionization quadrupole time of flight MS analyses were carried out with an Easy-nLC system (Proxeon; Thermo Scientific) coupled to a micrOTOF Q II MS device (Bruker Daltonics). For LC separation, a two-column setup with a C18 reverse phase for hydrophobic interaction of peptides was used: precolumn, Proxeon EASY-PreColumn (length = 2 cm, i.d. = 100 μm; ReproSil-Pur C18-AQ, 5 μm, 120 A); analytical column, Proxeon EASY-Column (length = 10 cm, i.d. = 75 μm; ReproSil-Pur C18-AQ, 3 μm, 120 A). The LC gradient started with 95% solution A (water + 0.1% formic acid), and the proportion of solution B (acetonitrile + 0.1% formic acid) was continuously increased for 10 min to 50% B. This ratio was applied for 3 min. Solution B was then continuously increased again for 20 min to 95% B and 5% A. MS/MS fragmentation was carried out automatically. For this, the software selected up to three peptides of highest intensity (with a minimal intensity of 3,000 counts) in the MS precursor scan.

For data processing, DataAnalysis software from Bruker Daltonics was used.

Database search was carried out with ProteinScape 2.0 (Bruker Daltonics) and the Mascot search engine in The Arabidopsis Information Resource (TAIR) 10 database (www.arabidopsis.org). The search was carried out with the following parameters: enzyme, trypsin/P, with up to one missed cleavage allowed; global modification, carbamidomethylation (C), variable modifications, acetyl (N), oxidation (M); precursor ion mass tolerance, 20 ppm; fragment ion mass tolerance, 0.05 D; peptide charge, 1+, 2+, and 3+; instrument type, electrospray ionization quadrupole time of flight. Minimum peptide length was set to 4, and protein and peptide assessments were carried out if the Mascot Score was greater than 25 (for proteins as well as peptides).

Proteins were further validated by comparison with the SUBA II database (Heazlewood et al., 2005, 2007) to determine the proportion of nonmitochondrial proteins in our sample (Supplemental Tables S2 and S3). Therefore, accession numbers of all identified proteins (according to the TAIR 10 database) were used for a search of the SUBA II database. Available proteomic data (MS and GFP data) given in SUBA II were used to assign each protein to its most likely subcellular localization. For four different data subsets (first hit proteins, unique proteins, all proteins, and all peptides), the subcellular distribution as well as the proportion of mitochondrial and nonmitochondrial proteins were determined (Supplemental Table S2).

Image Processing and Database Generation Using GelMap

Gels were scanned using the Image Scanner III (GE Healthcare) and stored as JPEG files with minimal compression. Image files were loaded into the Delta 2D 4.2 software package (Decodon). Spot detection was carried out by automatic mode of the software package and corrected manually. A file including the coordinates of all spots was generated (coord file) and exported into Excel (Microsoft). Finally, gel image (.jgp) and coord (.txt) files were exported into the GelMap software package available at www.gelmap.de (Rode et al., 2011). Information on how to use GelMap is given in the how-to area of the GelMap Web site (http://www.gelmap.de/howto). For the analyses of 2D BN gels, detailed information for all identified proteins was directly added to the coord file. As a consequence, the GelMap database for mitochondria of Arabidopsis only is based on two files.

Furthermore, an optional second table (.txt) file was uploaded that provides peptide data of the MS/MS analyses. Information about the identified peptides of a protein is available via a link for more peptide details in the pop-up windows on the reference gel (Fig. 4).

Supplemental Data

The following materials are available in the online version of this article.

Supplemental Figure S1. Assignment of subunits of complex V (ATP synthase).

Supplemental Figure S2. Protein complex visualization by GelMap.

Supplemental Table S1. Detail table of the 2D BN/SDS reference map for Arabidopsis mitochondrial proteins.

Supplemental Table S2. Subcellular localization of the identified proteins according to the SUBA II database.

Supplemental Table S3. SUBA II search results.

Note Added in Proof

The Arabidopsis mitochondrial protein complex proteome reference map (http://www.gelmap.de/arabidopsis_mito) was integrated into the Arabidopsis proteomics meta portal "MASCP Gator" (http://gator.mascproteomics.org/).

ACKNOWLEDGMENTS

We thank Dagmar Lewejohann for expert technical assistance and Holger Eubel for critically reading the manuscript.

Received June 23, 2011; accepted August 10, 2011; published August 12, 2011.

LITERATURE CITED

Arnold I, Pfeiffer K, Neupert W, Stuart RA, Schägger H (1998) Yeast mitochondrial F_1F_0-ATP synthase exists as a dimer: identification of three dimer-specific subunits. EMBO J **17:** 7170–7178

Baker MJ, Webb CT, Stroud DA, Palmer CS, Frazier AE, Guiard B, Chacinska A, Gulbis JM, Ryan MT (2009) Structural and functional requirements for activity of the Tim9-Tim10 complex in mitochondrial protein import. Mol Biol Cell **20:** 769–779

Braun HP, Emmermann M, Kruft V, Schmitz UK (1992) The general mitochondrial processing peptidase from potato is an integral part of cytochrome c reductase of the respiratory chain. EMBO J **11:** 3219–3227

Braun HP, Schmitz UK (1995) The bifunctional cytochrome c reductase/processing peptidase complex from plant mitochondria. J Bioenerg Biomembr **27:** 423–436

Bykova NV, Egsgaard H, Møller IM (2003a) Identification of 14 new phosphoproteins involved in important plant mitochondrial processes. FEBS Lett **540:** 141–146

Bykova NV, Stensballe A, Egsgaard H, Jensen ON, Møller IM (2003b) Phosphorylation of formate dehydrogenase in potato tuber mitochondria. J Biol Chem **278:** 26021–26030

Carroll J, Shannon RJ, Fearnley IM, Walker JE, Hirst J (2002) Definition of the nuclear encoded protein composition of bovine heart mitochondrial complex I: identification of two new subunits. J Biol Chem **277:** 50311–50317

Delannoy E, Stanley WA, Bond CS, Small ID (2007) Pentatricopeptide repeat (PPR) proteins as sequence-specificity factors in post-transcriptional processes in organelles. Biochem Soc Trans **35:** 1643–1647

Douce R, Bourguignon J, Neuburger M, Rébeillé F (2001) The glycine decarboxylase system: a fascinating complex. Trends Plant Sci **6:** 167–176

Emmermann M, Braun HP, Schmitz UK (1991) The ADP/ATP translocator from potato has a long amino-terminal extension. Curr Genet **20:** 405–410

Eubel H, Jänsch L, Braun HP (2003) New insights into the respiratory chain of plant mitochondria: supercomplexes and a unique composition of complex II. Plant Physiol **133:** 274–286

Giegé P, Sweetlove LJ, Leaver CJ (2003) Identification of mitochondrial protein complexes in Arabidopsis using two-dimensional blue-native polyacrylamide gel electrophoresis. Plant Mol Biol Rep **21:** 133–144

Halperin T, Zheng B, Itzhaki H, Clarke AK, Adam Z (2001) Plant mitochondria contain proteolytic and regulatory subunits of the ATP-dependent Clp protease. Plant Mol Biol **45:** 461–468

Heazlewood JL, Howell KA, Millar AH (2003a) Mitochondrial complex I from Arabidopsis and rice: orthologs of mammalian and fungal components coupled with plant-specific subunits. Biochim Biophys Acta **1604:** 159–169

Heazlewood JL, Howell KA, Whelan J, Millar AH (2003b) Towards an analysis of the rice mitochondrial proteome. Plant Physiol **132:** 230–242

Heazlewood JL, Tonti-Filippini JS, Gout AM, Day DA, Whelan J, Millar AH (2004) Experimental analysis of the *Arabidopsis* mitochondrial proteome highlights signaling and regulatory components, provides assessment of targeting prediction programs, and indicates plant-specific mitochondrial proteins. Plant Cell **16:** 241–256

Heazlewood JL, Tonti-Filippini J, Verboom RE, Millar AH (2005) Combining experimental and predicted datasets for determination of the subcellular location of proteins in Arabidopsis. Plant Physiol **139:** 598–609

Heazlewood JL, Verboom RE, Tonti-Filippini J, Small I, Millar AH (2007) SUBA: the Arabidopsis subcellular database. Nucleic Acids Res **35:** D213–D218

Heazlewood JL, Whelan J, Millar AH (2003c) The products of the mitochondrial orf25 and orfB genes are FO components in the plant F1FO ATP synthase. FEBS Lett **540:** 201–205

Heinemeyer J, Scheibe B, Schmitz UK, Braun HP (2009) Blue native DIGE as a tool for comparative analyses of protein complexes. J Prot **72:** 539–544

Huang S, Taylor NL, Narsai R, Eubel H, Whelan J, Millar AH (2010) Functional and composition differences between mitochondrial complex II in Arabidopsis and rice are correlated with the complex genetic history of the enzyme. Plant Mol Biol **72:** 331–342

Jänsch L, Kruft V, Schmitz UK, Braun HP (1996) New insights into the composition, molecular mass and stoichiometry of the protein complexes of plant mitochondria. Plant J **9:** 357–368

Jänsch L, Kruft V, Schmitz UK, Braun HP (1998) Unique composition of the preprotein translocase of the outer mitochondrial membrane from plants. J Biol Chem **273:** 17251–17257

Jenner HL, Winning BM, Millar AH, Tomlinson KL, Leaver CJ, Hill SA (2001) NAD malic enzyme and the control of carbohydrate metabolism in potato tubers. Plant Physiol **126:** 1139–1149

Klodmann J, Braun HP (2011) Proteomic approach to characterize mitochondrial complex I from plants. Phytochemistry **72:** 1071–1080

Klodmann J, Sunderhaus S, Nimtz M, Jänsch L, Braun HP (2010) Internal architecture of mitochondrial complex I from *Arabidopsis thaliana*. Plant Cell **22:** 797–810

Kruft V, Eubel H, Werhahn WH, Jänsch L, Braun HP (2001) Proteomic approach to identify novel mitochondrial functions in *Arabidopsis thaliana*. Plant Physiol **127:** 1694–1710

Lee CP, Eubel H, O'Toole N, Millar AH (2011) Combining proteomics of root and shoot mitochondria and transcript analysis to define constitutive and variable components in plant mitochondria. Phytochemistry **72:** 1092–1108

Lister R, Carrie C, Duncan O, Ho LH, Howell KA, Murcha MW, Whelan J (2007) Functional definition of outer membrane proteins involved in preprotein import into mitochondria. Plant Cell **19:** 3739–3759

Lister R, Hulett JM, Lithgow T, Whelan J (2005) Protein import into mitochondria: origins and functions today. Mol Membr Biol **22:** 87–100

Meyer EH, Heazlewood JL, Millar AH (2007) Mitochondrial acyl carrier proteins in Arabidopsis thaliana are predominantly soluble matrix proteins and none can be confirmed as subunits of respiratory complex I. Plant Mol Biol **64:** 319–327

Meyer EH, Taylor NL, Millar AH (2008) Resolving and identifying protein components of plant mitochondrial respiratory complexes using three dimensions of gel electrophoresis. J Proteome Res **2:** 786–794

Michalecka AM, Svensson AS, Johansson FI, Agius SC, Johanson U, Brennicke A, Binder S, Rasmusson AG (2003) Arabidopsis genes encoding mitochondrial type II NAD(P)H dehydrogenases have different evolutionary origin and show distinct responses to light. Plant Physiol **133:** 642–652

Millar AH, Eubel H, Jänsch L, Kruft V, Heazlewood L, Braun HP (2004a) Mitochondrial cytochrome c oxidase and succinate dehydrogenase contain plant-specific subunits. Plant Mol Biol **56:** 77–89

Millar AH, Mittova V, Kiddle G, Heazlewood JL, Bartoli CG, Theodoulou FL, Foyer CH (2003) Control of ascorbate synthesis by respiration and its implications for stress responses. Plant Physiol **133:** 443–447

Millar AH, Sweetlove LJ, Giegé P, Leaver CJ (2001) Analysis of the Arabidopsis mitochondrial proteome. Plant Physiol **127:** 1711–1727

Millar AH, Trend AE, Heazlewood JL (2004b) Changes in the mitochondrial proteome during the anoxia to air transition in rice focus around cytochrome-containing respiratory complexes. J Biol Chem **279:** 39471–39478

Mozo T, Fischer K, Flügge UI, Schmitz UK (1995) The N-terminal extension of the ADP/ATP translocator is not involved in targeting to plant mitochondria in vivo. Plant J **7:** 1015–1020

Neuhoff V, Arold N, Taube D, Ehrhardt W (1988) Improved staining of proteins in polyacrylamide gels including isoelectric focusing gels with clear background at nanogram sensitivity using Coomassie Brilliant Blue G-250 and R-250. Electrophoresis **6:** 255–262

Peltier JB, Ripoll DR, Friso G, Rudella A, Cai Y, Ytterberg J, Giacomelli L,

Pillardy J, van Wijk KJ (2004) Clp protease complexes from photosynthetic and non-photosynthetic plastids and mitochondria of plants, their predicted three-dimensional structures, and functional implications. J Biol Chem **279:** 4768–4781

Peters K, Dukina NV, Jänsch L, Braun HP, Boekema EJ (2008) A structural investigation of complex I and I+III_2 supercomplex from Zea mays at 11-13 Å resolution: assignment of the carbonic anhydrase domain and evidence for structural heterogeneity within complex I. Biochim Biophys Acta (Bioenergetics) **1777:** 84–93

Rasmusson AG, Agius SC (2001) Rotenone-insensitive NAD(P)H dehydrogenases in plants: immunodetection and distribution of native proteins in mitochondria. Plant Physiol Biochem **39:** 1057–1066

Rode C, Senkler M, Klodmann J, Winkelmann T, Braun HP (2011) GelMap: a novel software tool for the creation and presentation of proteome reference maps. J Proteomics **74:** 2214–2219

Schägger H, von Jagow G (1987) Tricine-sodium dodecyl sulfate-polyacrylamide gel electrophoresis for the separation of proteins in the range from 1 to 100 kDa. Anal Biochem **166:** 368–379

Schägger H, von Jagow G (1991) Blue native electrophoresis for isolation of membrane protein complexes in enzymatically active form. Anal Biochem **199:** 223–231

Sunderhaus S, Dudkina N, Jänsch L, Klodmann J, Heinemeyer J, Perales M, Zabaleta E, Boekema E, Braun HP (2006) Carbonic anhydrase subunits form a matrix-exposed domain attached to the membrane arm of mitochondrial complex I in plants. J Biol Chem **281:** 6482–6488

Sunderhaus S, Klodmann J, Lenz C, Braun HP (2010) Supramolecular structure of the OXPHOS system in highly thermogenic tissue of Arum maculatum. Plant Physiol Biochem **48:** 265–272

Taylor N, Heazlewood J, Millar AH (2011) The Arabidopsis thaliana 2D gel mitochondrial proteome: refining the value of reference maps for assessing protein abundance, contaminants and post-translational modifications. Proteomics **11:** 1720–1733

Van Aken O, Whelan J, van Breusegem F (2010) Prohibitins: mitochondrial partners in development and stress response. Trends Plant Sci **15:** 275–282

Werhahn WH, Braun HP (2002) Biochemical dissection of the mitochondrial proteome of Arabidopsis thaliana by three-dimensional gel electrophoresis. Electrophoresis **23:** 640–646

Werhahn WH, Jänsch L, Braun HP (2003) Identification of novel subunits of the TOM complex from Arabidopsis thaliana. Plant Physiol Biochem **41:** 407–416

Werhahn WH, Niemeyer A, Jänsch L, Kruft V, Schmitz UK, Braun HP (2001) Purification and characterization of the preprotein translocase of the outer mitochondrial membrane from *Arabidopsis thaliana*: identification of multiple forms of TOM20. Plant Physiol **125:** 943–954

Winning BM, Sarah CJ, Purdue PE, Day CD, Leaver CJ (1992) The adenine nucleotide translocator of higher plants is synthesized as a large precursor that is processed upon import into mitochondria. Plant J **2:** 763–773

Wittig I, Braun HP, Schägger H (2006) Blue-native PAGE. Nat Protoc **1:** 418–428

Zhou ZH, McCarthy DB, O'Connor CM, Reed LJ, Stoops JK (2001) The remarkable structural and functional organization of the eukaryotic pyruvate dehydrogenase complexes. Proc Natl Acad Sci USA **98:** 14802–14807